http://dx.doi.org/10.5516/NET.09.2010.066

ASSESSMENT OF POSSIBILITY OF PRIMARY WATER STRESS CORROSION CRACKING OCCURRENCE BASED ON RESIDUAL STRESS ANALYSIS IN PRESSURIZER SAFETY NOZZLE OF NUCLEAR POWER PLANT

KYOUNG-SOO LEE[1,*], W. KIM[2], and JEONG-GEUN LEE[2]
[1]System Engineering Laboratory, KHNP Central Research Institute
Daejeon, 305-343, Korea
[2]Nuclear Power Generation Laboratory, Korea Electric Power Research Institute
Daejeon, 305-380, Korea
[*]Corresponding author. E-mail : leekys@khnp.co.kr

Received December 06, 2010
Accepted for Publication July 26, 2011

Primary water stress corrosion cracking (PWSCC) is a major safety concern in the nuclear power industry worldwide. PWSCC is known to initiate only in the condition in which sufficiently high tensile stress is applied to alloy 600 tube material or alloy 82/182 weld material in pressurized water reactor operating environments. However, it is still uncertain how much tensile stress is re-quired to generate PWSCC or what causes such high tensile stress. This study was performed to pre-dict the magnitude of weld residual stress and operating stress and compare it with previous experi-mental results for PWSCC initiation. For the study, a pressurizer safety nozzle was selected because it is reported to be vulnerable to PWSCC in overseas plants. The assessment was conducted by nu-merical analysis. Before performing stress analysis for plant conditions, a preliminary mock-up ana-lysis was done. The result of the preliminary analysis was validated by residual stress measurement in the mock-up. After verification of the analysis methodology, an analysis under plant conditions was conducted. The analysis results show that the stress level is not high enough to initiate PWSCC. If a plant is properly welded and operated, PWSCC is not likely to occur in the pressurizer safety nozzle.

KEYWORDS : Dissimilar Metal Weld, Finite Element Analysis, Primary Water Stress Corrosion Cracking, Residual Stress Measurement, Weld Residual Stress

1. INTRODUCTION

Since 1994, more than 300 dissimilar metal welds (DMW) using alloy 82/182 in over 30 pres-surized water reactor (PWR) plants have experienced primary water stress corrosion cracking (PWSCC) during their operation time after between 53,400 and 180,000 effective full power hours (EFPH) [1].

So far, PWSCC is known to be related to combination of particular material, environmental and stress conditions as shown in Fig. 1. It is known to occur only in nickel base alloy 600, alloy 82 or 182 which has been in service in PWRs in the primary water condition (high temperature of more than 300ºC, high pressure of more than 15 MPa, oxygen concentration, etc.) and tensile stress state. Extensive studies have been conducted to understand residual stress conditions in the various weld regions of nuclear power plants [2-7]. However, it is still uncertain how much tensile stress is required to initiate PWSCC or what causes such high tensile stress. Recently EPRI (Electric Power Research

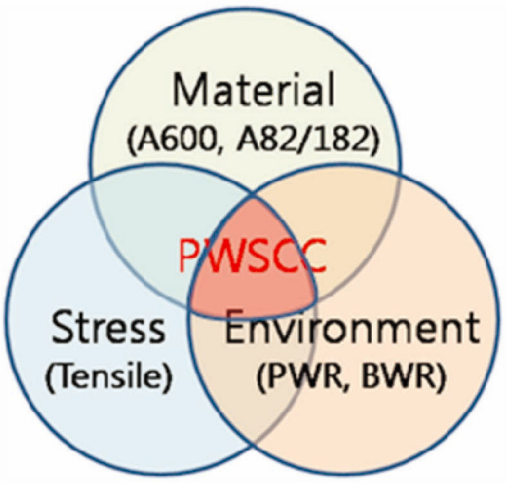

Fig. 1. Condition of PWSCC Occurrence

Institute) issued a report [1] and reported experimental results for PWSCC initiation stress as shown in Fig. 2.

This study was started to confirm that weld residual stress can reach PWSCC initiation stress lev-els as suggested in the reference [1]. PWSCC usually occurs on the inner surface of weld regions which come into contact with pressurized high temperature water coolant. However, it is nearly impossible to measure the residual stress on the inner surfaces of pipes or nozzles in operating nuclear power plants because of high radiation and inaccessibility. Current residual stress measurement technologies have many limitations. Various measurement techniques other than the neutron diffraction method can measure the stress only within about 2 mm depth from the surface of the material, while the neutron diffraction method can be used only in facilities that have nuclear reactors. Accordingly, residual stress evaluation for through thickness and inner surface has to rely on finite element analysis (FEA). However, FEA results can vary according to the modeling and analysis process, so FEA results should be verified by experiment. For the verification of FEA, a mock-up was fabricated. The pressurizer safety nozzle was selected for the mock-up because it is known to be highly susceptible to PWSCC because of its high operating temperature. Numerical analysis and measurement for the mock-up were per-formed and verified with each other. After the verification of FEA, the final analysis of residual stress under plant conditions was conducted.

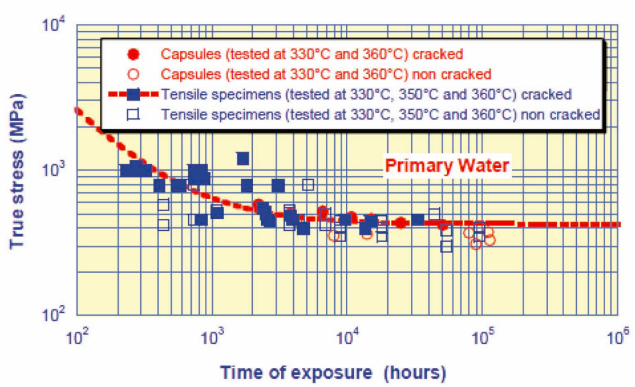

Fig. 2. PWSCC Initiation Stresses as a Function of Time [1]

2. MOCK-UP FABRICATION

A mock-up of weld parts of a pressurizer safety nozzle was fabricated. Material and dimensional conditions of the mock-up were identical to those of a nuclear power plant. Figure 3 shows the configuration of the mock-up, and Table 1shows the typical material properties of each part at the ambient temperature.

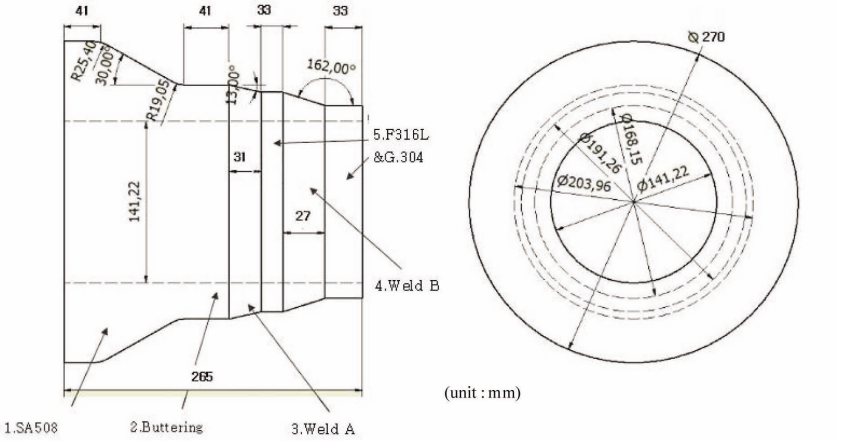

Fig. 3. Configuration of the Mock-up

Table 1. Material Properties of Mock-up at 20 °C

	Tensile strength (MPa)	Yield strength (MPa)	Thermal expansion coeff. ($^oC^{-1}$)	Thermal conductivity ($Wm^{-1}{}^oC^{-1}$)
SA508 (Nozzle)	609.7	479.4	1.15×10^{-5}	40.7
Alloy 82/182 (Weld A)	658.3	393.7	1.22×10^{-5}	14.9
S/S F316L (SE)	482.6	203	1.53×10^{-5}	14.2
S/S TP304 (pipe)	517.1	243.6	1.53×10^{-5}	14.9

The mock-up was composed of three parts: an SA508 forged nozzle, an F316L safe-end, and a Type 304 stainless steel pipe. It had two welds, one for dissimilar metal weld (DMW) between the carbon steel nozzle and the stainless steel safe end, and the other for similar metal weld (SMW) be-tween the stainless steel safe end and stainless steel pipe. Prior to fabrication of the DMW, the forged nozzle was buttered with about a 5 mm thick layer of alloy 182. The DMW and SMW were fabricat-ed sequentially. The first three passes of DMW were welded by gas tungsten arc welding (GTAW) using alloy 82 and the remaining passes by shielded metal arc welding (SMAW) using alloy 182. Figure 4 shows the welding passes.

All welding was manually done in accordance with the welding procedure used in the plant. The welding time for every pass was recorded to calculate the heat input. The inter-pass temperature was strictly kept below 175ºC as per welding procedure. Table 2 shows the main welding parameters used.

During the welding, the mock-up was placed on a working table and the contact point was spot-welded to the table along the periphery of the nozzle face, allowing the other parts to deform freely.

3. VERIFICATION OF WELD RESIDUAL STRESS ANALYSIS WITH MEASUREMENT

3.1 FE Model for Mock-up

Axisymmetric FE models were developed to simulate thermo-mechanical behavior of the nozzle mock-up as shown in Fig. 5. In Model A, DMW with buttering was included. In Model B, SMW was added to Model A. Two separate models were developed sequentially to independently observe the effect of DMW and SMW on the stress states in the DMW region.

Approximately 1900 linear 4-node continuum elements were used in Model A, and 2500 ele-ments were used in

Table 2. Weld Parameters for Mock-up Fabrication

	Weld rod (mm)	Current (A)	Voltage (V)	Polarity	Shield gas
GTAW	2.4	120~140	12	DCRP	Ar (99.99%)
SMAW	3.2	130~140	25		

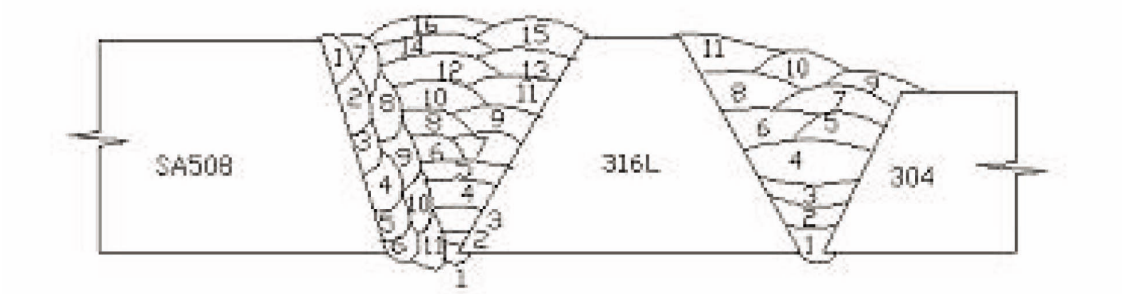

Fig. 4. Welding Sequence for Mock-up Fabrication

(a) Model A for Buttering + DMW

(b) Model B for Buttering + DMW + SMW

Fig. 5. Models for Finite Element Analysis

Model B. Figure 6 shows the mesh of Model B for the mock-up.

Since effects of weld sequence and direction significantly affect the final residual stress distribu-tion [8, 9], modeling and analysis were performed applying the actual multi-pass weld sequence and direction using the 'model change' option of ABAQUS software [10] as shown in Fig. 7.

A sequentially-coupled thermal-stress analysis approach was adopted. Thermal boundary condi-tion included convective heat loss from the nozzle surface, but radiation heat loss was not considered since its effect on residual stresses was negligible.

As the mock-up was spot-welded to a working table as mentioned earlier, the outermost points of the nozzle face in the analysis model were assumed to be fixed as shown in Fig. 8.

3.2 Weld Residual Stress Analysis of the Mock-up

Through thermal and structural analyses, weld residual stresses were estimated. During welding, materials experience temperature change from ambient temperature to melting temperature. For the weld residual stress analysis, material properties from ambient temperature to melting temperature are needed. Material properties for the weld analysis were obtained from [11] and are shown in Fig. 9(a) ~ 9(e). For the thermal analysis, conduction was applied between the base material and the weld metal, whereas convection was applied between the mock-up and ambient air. Radiation effect was ignored. In the structural analysis, the isotropic hardening model provided in ABAQUS software was applied for the behavior of the elastic-plastic region. From the analysis, the residual stresses in axial and cir-cumferential directions were plotted in Figs. 10(a) to 10(d). As shown in the legend, the highest tensile stress represents 500 MPa in red color, while the highest compressive stress represents (-)500 MPa in dark blue.

Axial stresses in both Models A and B show that tensile stresses were widely distributed in the outer region of the nozzle wall, whereas compressive or low tensile stresses

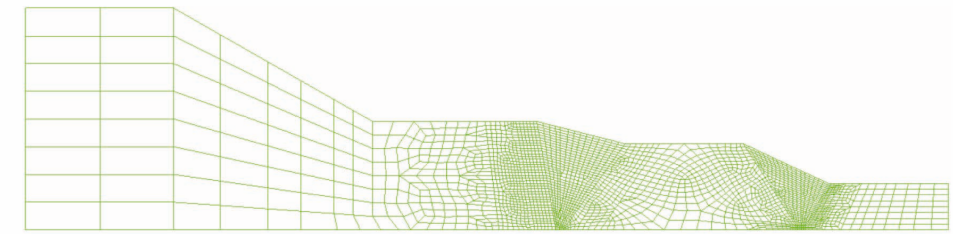

Fig. 6. Element Mesh of Model B

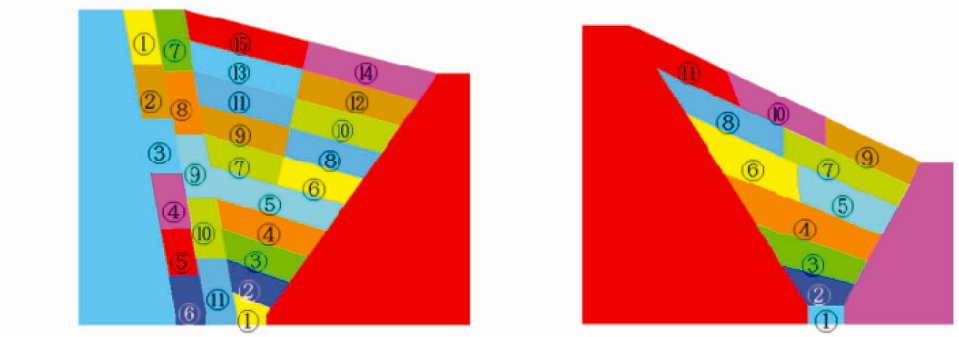

Fig. 7. Weld Sequence and Direction in the Analysis

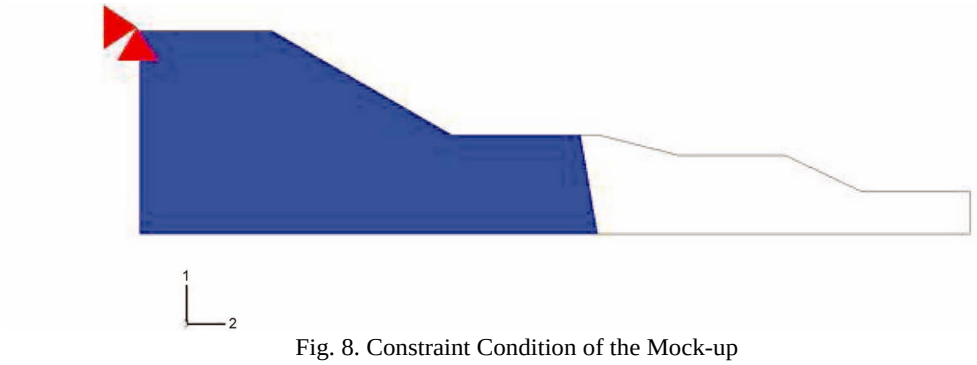

Fig. 8. Constraint Condition of the Mock-up

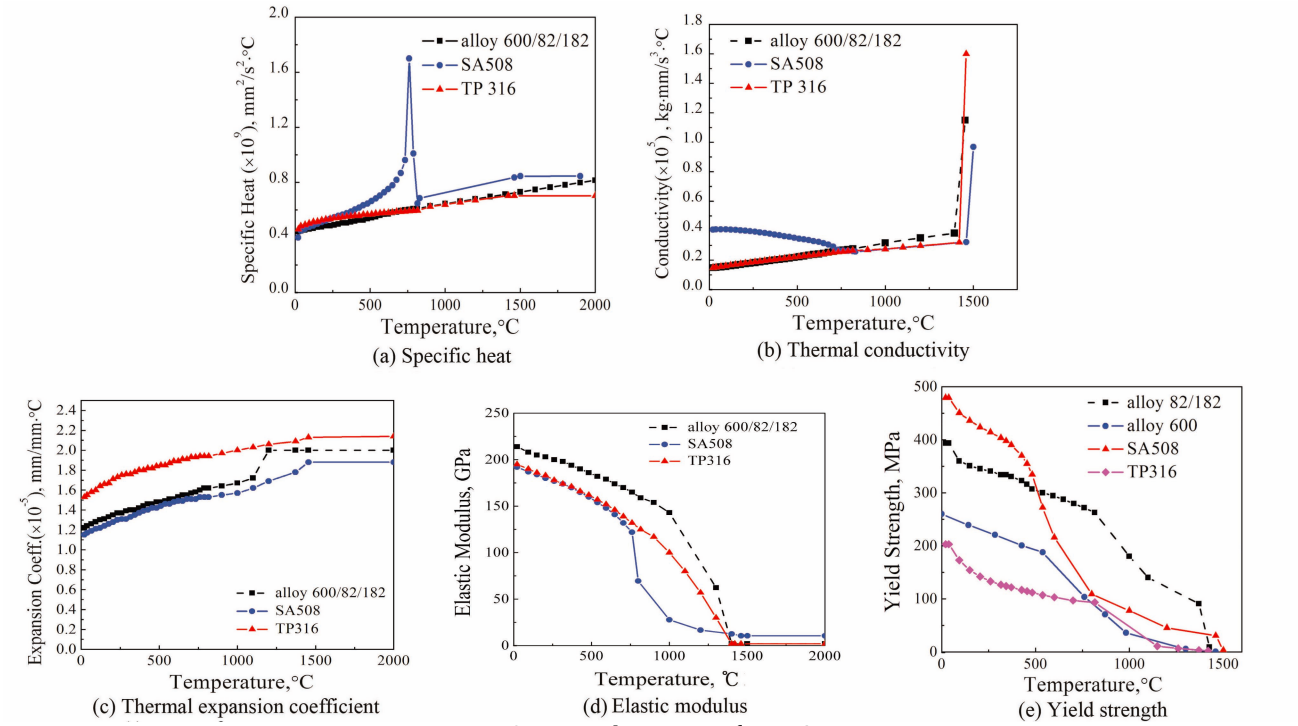

Fig. 9. Material Properties for FEA

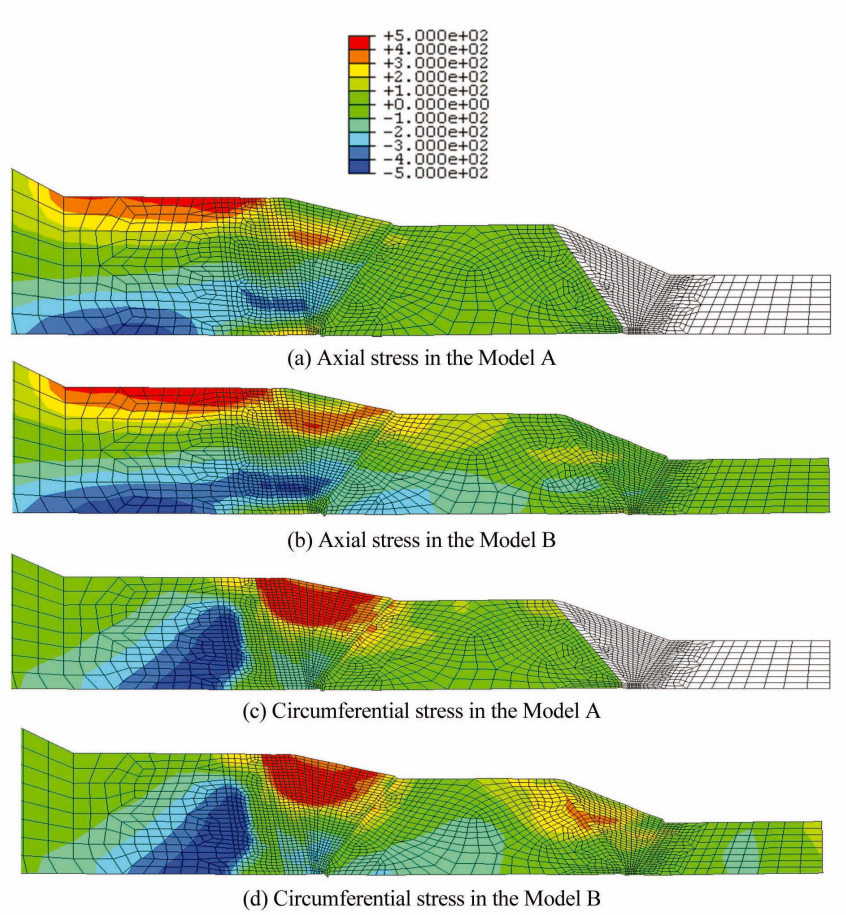

Fig. 10. Weld Residual Stress Distribution in the Mock-up

were distributed in the inner region of the wall. Similarly circumferential stresses in both Models A and B show that tensile stresses were widely distributed in the outer region of the wall, whereas compressive stresses were distributed in the inner region of the wall. It was observed that both axial and circumferential stresses at the inner surface of DMW region revealed a more compressive state due to effect of SMW. Later, it would be more clearly shown in Fig. 17. This implies that the residual stress state can be changed by neighboring welds.

For further assessment, the residual stresses from FE analysis were selectively collected along the paths A, B, and C as shown in Fig. 13. Path A ran along the inner surface of the mock-up, from a point (62.5 mm away from the nozzle side from the left corner of DMW's 1st bead), to the end of the safe-end. Path B ran along the radial direction along the DMW center line, beginning at a point on the inner surface to the outer surface. Path C (#1 to ~#5) represents the outer surface of the mock-up, corresponding to the points where residual stresses were measured for comparison.

3.3 Residual Stress Measurement for the Mock-up

For verification of FEA, residual stress measurement for the mock-up was conducted. The hole-drilling method (HDM) was used [12]. HDM is known as the most reliable technology among the currently available methods. Residual stresses can be calculated using the measured strains when a hole is drilled in the center of a rosette type strain gauge attached to the mock-up. Stresses and their directions can be calculated by the following equations (1) ~ (4):

$$\sigma_{max}, \sigma_{min} = (\varepsilon_1 + \varepsilon_3)/4A \pm (\sqrt{2}/4B) \left[(\varepsilon_1 - \varepsilon_2)^2 + (\varepsilon_2 - \varepsilon_3)^2\right]^{1/2}, \quad (1)$$

$$\beta = (1/2)\tan^{-1}\left[(\varepsilon_3 - 2\varepsilon_2 + \varepsilon_1)/(\varepsilon_3 - \varepsilon_1)\right], \quad (2)$$

where σ_{max}, σ_{min} are the principal stresses; β is the angle measured clockwise from the axis of gauge 1 to the maximum principal stress direction; and ε_1, ε_2, ε_3 are the relaxed strains measured in strain gauges 1, 2 and 3. Here, A and B are constants given by the following relations:

$$A = -a(1+\nu)/2E, \quad (3)$$

$$B = -b/2E, \quad (4)$$

where E and ν are Young's modulus and Poisson's ratio of the material, and a and b are the dimensionless, almost material-independent constants[12]. Once σ_{max}, σ_{min} and β are obtained, the axial and circumferential stresses can be calculated. Figure 11 shows a typical rosette type strain gauge.

Strains were measured at five locations along path C shown in figure 12 for the verification of the results of FEA. The measurement locations were selected for convenience. Although the inner surface of weld region is more important from the viewpoint of PWSCC, it is impossible to attach strain gauges to the inner surface of the mock-up nozzle. For the verification purpose of FEA, it is sufficient to measure the stress at the outer surface. The distance between gauges was maintained to more than 15 mm to avoid interference from neighboring gauges. Table 3 summarizes the principal stresses, that is, axial and circumferential stresses, calculated from the strain measurement results.

The axial and circumferential stresses from measurement were compared with those from FE analysis for model B as shown in Fig. 13. Considering that the general measurement error of HDM is around 20 to 50 MPa [13], the measured data and FEA results seem to be in a good

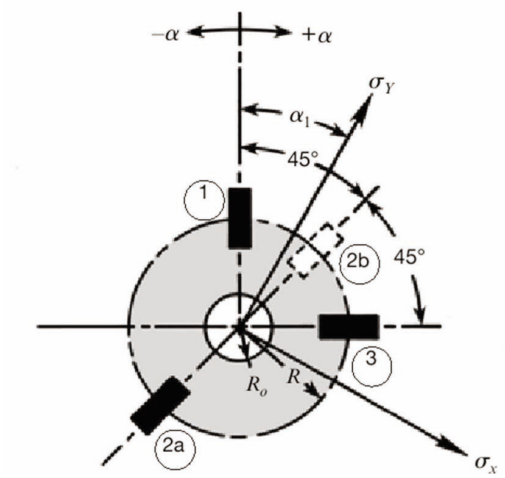

Fig. 11. Strain Rosette Gauge Type used for Measurement

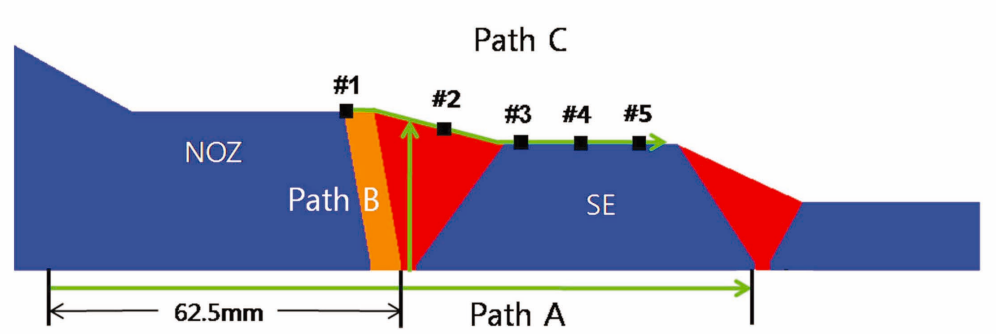

Fig. 12. Path Set for Data Acquisition

agreement. Through this comparison, the FEA methodology used in this study is confirmed to be adequate and reliable.

4. WELD RESIDUAL STRESS ANALYSIS FOR PLANT CONDITION

After verification of the FEA methodology through mock-up measurement, residual stress analy-sis was re-performed under plant conditions. The constraint conditions during welding of the pres-surizer safety nozzle in the plant are slightly different from those of mock-up fabrication. In the actual case, DMW (safe-end to pressurizer safety nozzle) was completed in the shop with the nozzle side fully constrained. Then SMW (the safe-end to piping) was performed in the plant with both ends fully constrained. Figures 14(a) and 14(b) show the actual constraint conditions of the pressurizer safety nozzle during DMW and SMW, respectively.

The other difference between the mock-up and the plant is post-weld heat treatment (PWHT) after buttering. To relieve the weld residual stresses generated in buttering, PWHT is normally performed in the actual pressurizer nozzle. But PWHT after buttering was not performed for mock-up fabrication to save cost and time.

The weld residual stresses obtained from FE analysis

Table 3. Measured Residual Stress on the Surface of the Mock-up

No.	σ_{max} (MPa)	σ_{min} (MPa)	Cir. St (MPa)	Axial St. (MPa)
#1	367	224	239	352
#2	308	159	307	159
#3	260	192	194	258
#4	150	5	86	70
#5	234	36	174	96

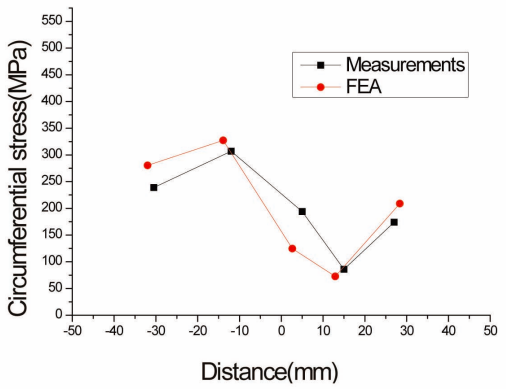

(a) Circumferential weld residual stress

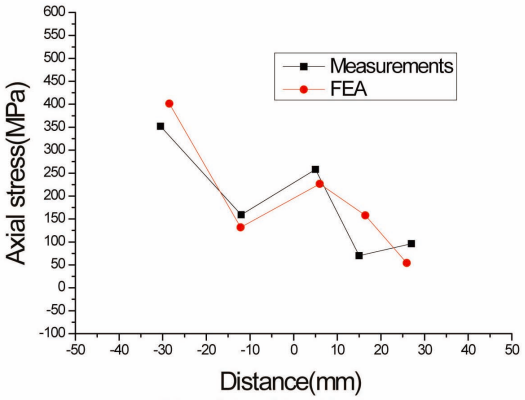

(b) Axial weld residual stress

Fig. 13. Comparison of the Results of Measurements and FEA Along Path C


(a) DMW in the shop

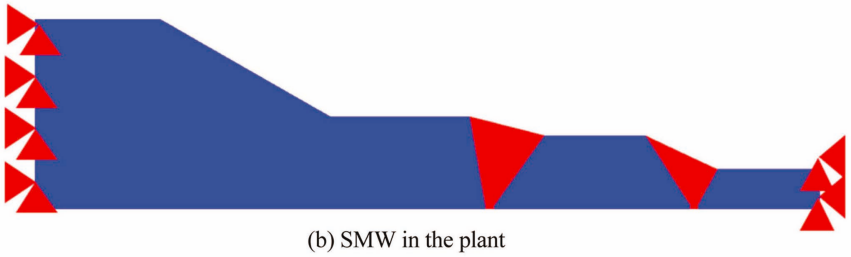
(b) SMW in the plant

Fig. 14. Constraint Condition in the Field

considering the actual plant conditions (con-straints and PWHT) are shown in Figs. 15(a) and 15(b) for axial stress and circumferential stress, respectively.

The residual axial stress through the nozzle wall in DMW shows a local bending stress distribu-tion: low tensile stress at the inner surface, compressive stress in the lower middle wall, high tensile stress in the upper middle wall, and low tensile stress again as it goes to the outer surface. The highest tensile stress is found in the upper middle of the thickness. However, the circumferential stress dis-tribution through the nozzle wall in DMW shows global bending with compressive state in the inner region and tensile state in the outer region.

Tensile stresses higher than the material yield strength are observed in the DMW region and its vicinity. Residual stresses exceeding material yield strength occur if thermal strain induced by cooling after welding is greater than the yield strain [9, 14]. The thermal strains induced in the nozzle, DMW, safe end, and pipe were found to be greater than the yield strains of the respective materials [14, 15]. Since the yield strength of the nozzle (SA508) is the greatest value among the mock-up materials, it is expected that the maximum residual tensile stress is located in the nozzle area despite the fact that it is somewhat affected by constraint conditions.

Comparing the plant conditions in Fig. 15(a) and 15(b) with mock-up fabrication conditions in Figs. 10(b) and 10(d), there is no significant difference in the magnitude and distribution of stresses around the DMW region. However, it is noted that the tensile axial stress around the SMW region is considerably increased, probably due to the constrained condition in the piping side.

During plant operation, high temperature and high pressure are applied to the weld, and they can affect the stress condition. It is known that hydrostatic pressure testing during plant start-up can affect the residual stress. To know those effects of residual stress in the weld region, further analysis was performed including hydrostatic testing and operating temperature-pressure conditions.

The hydrostatic test condition of 25ºC and 21.5 MPa and operating conditions of 354ºC and 15.5 MPa were applied to the analysis. The analysis for the hydrostatic test condition was first performed and the analysis for the operating condition followed. It was assumed that temperature increased over 48 hours. The stress data were obtained after 1,000,000 seconds which were considered as a stable condition. The results are shown in Figs. 16 and 17. For comparison, the results from three conditions of weld, hydrostatic test, and operation are included in the figures. Figure 16 shows axial residual stress, and figure 17 shows circumferential residual stress. They show that the stress conditions were changed by hydrostatic testing and normal operation conditions, but the degree of change was not significant.

5. RESULTS AND DISCUSSIONS

PWSCC usually initiates on the inner surface of the DMW region in reactor coolant piping which is in contact with primary water of high pressure and temperature. Once initiated, it grows through the wall thickness and causes reactor coolant leakage when the crack penetrates the wall. From the view-point of crack initiation and growth, stress

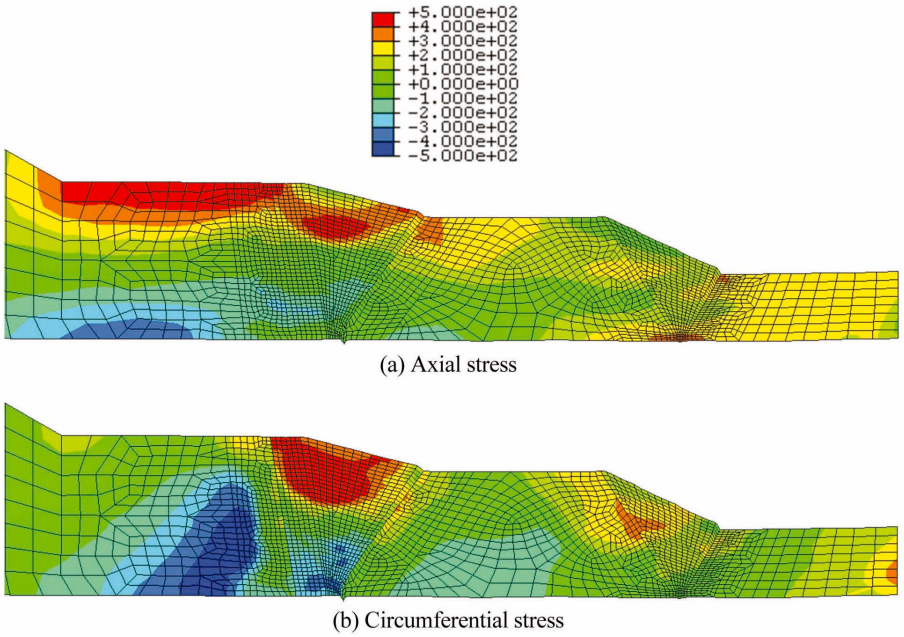

(a) Axial stress

(b) Circumferential stress

Fig. 15. Weld Residual Stress Distribution Inunder Plant Conditions

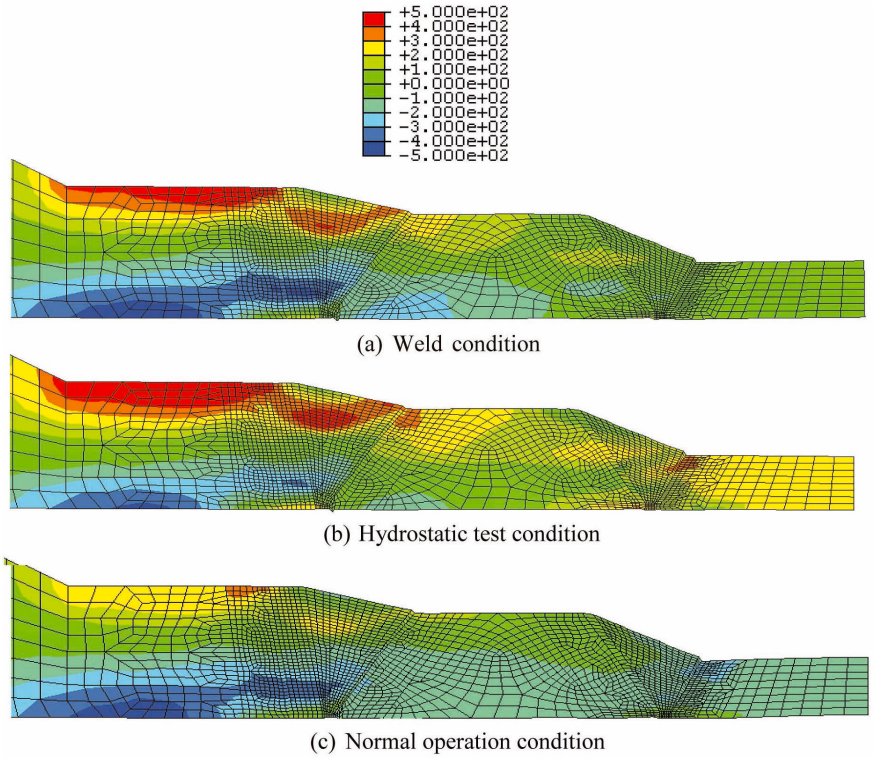

(a) Weld condition

(b) Hydrostatic test condition

(c) Normal operation condition

Fig. 16. Change of Axial Residual Stress Distribution

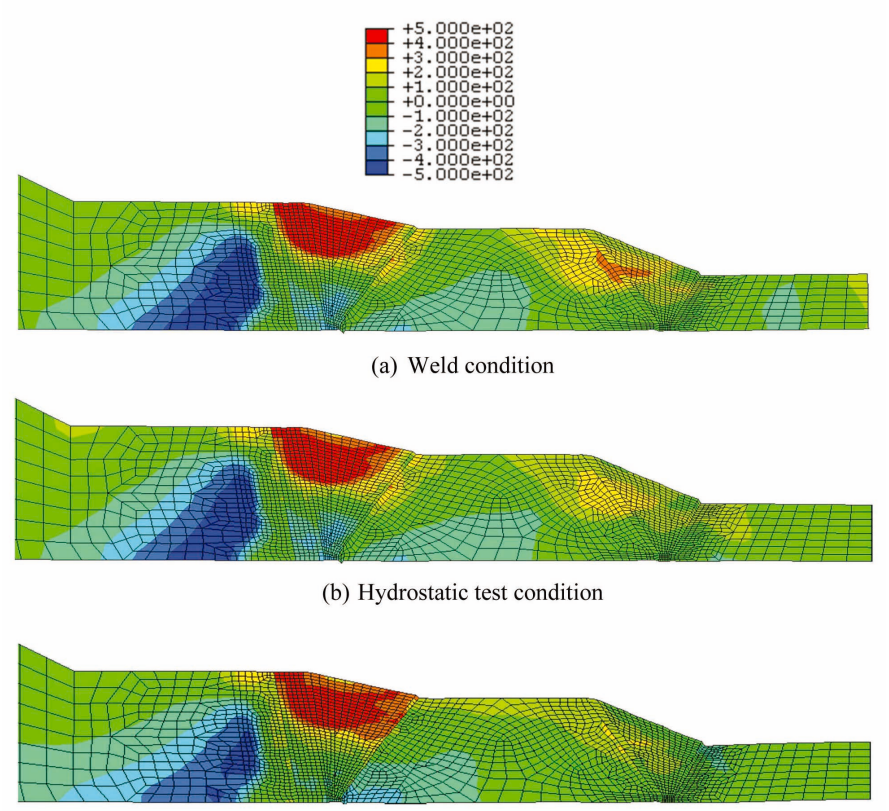

(a) Weld condition

(b) Hydrostatic test condition

(c) Normal operation condition

Fig. 17. Change of Circumferential Residual Stress Distribution

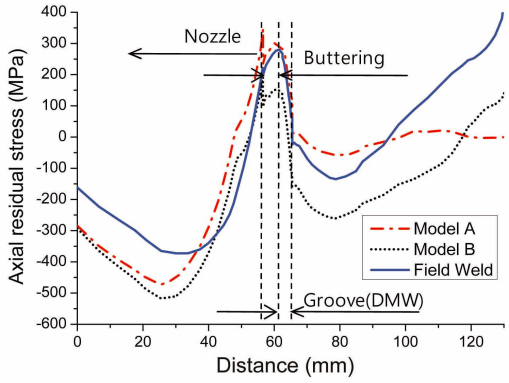

(a) Axial stress

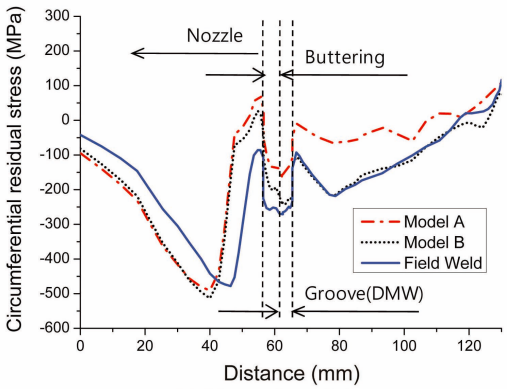

(b) Circumferential stress

Fig. 18. Weld Residual Stress Distribution on Inner Surface

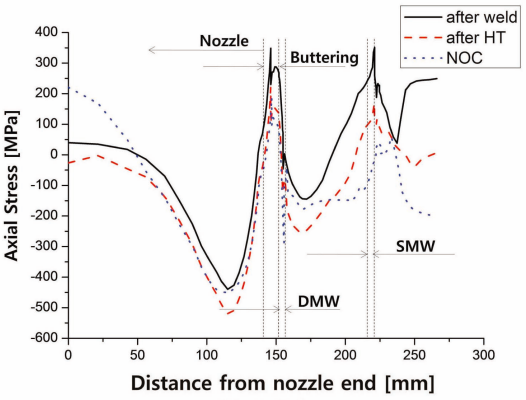

(a) Axial stress

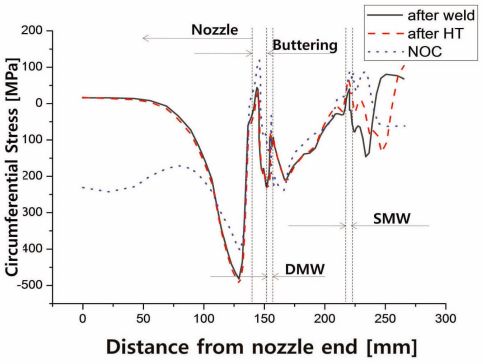

(b) Circumferential stress

Fig. 19. Change of Stress Distribution on Inner Surface

profiles of the inner surface and through-thickness are more important. In particular, axial tensile stress may cause circumferential crack initiation and growth, while circumferential tensile stress may cause axial crack initiation and growth. On the contrary, compressive stress may act as a crack closing force resulting in a beneficial effect on PWSCC.

Fig. 18 shows the weld residual stress distribution on the inner surface of the pressurizer safety nozzle (along path A in Fig. 12) for Models A and B and plant constraint conditions. The axial residual stress on the inner surface in buttering and the DMW region decreased due to neighboring SMW weld and increased again in the field weld. The increase of axial stress by the field weld is considered to be due to the increase of axial constraint. In contrast to the axial stress, the circumferen-tial stress on the inner surface of buttering and the DMW region was decreased by neighboring SMW weld and decreased again in the field weld. The decrease of circumferential stress by the field weld is considered to be due to post-welding heat treatment. The circumferential constraint condition in the field weld was same with that of the mock-up weld. The maximum tensile weld residual stress was about 280 MPa in the axial direction.

Figure 19 shows the stress distribution on the inner surface of the pressurizer safety nozzle (along path A in Fig. 12) after hydrostatic testing and normal operation. The axial residual stress on the inner surface in buttering and the DMW region was decreased by hydrostatic testing and normal operating conditions. The maximum axial tensile stress in buttering and the DMW region in normal operation conditions was about 190 MPa in buttering. In contrast to the axial stress, the circumferential stress on the inner surface of buttering and the DMW region did not change much as a result of hydrostatic testing, and it increased in normal operating conditions. The maximum circumferential tensile stress was about 110 MPa in the buttering region. According to the analysis results, circumferential cracking is more likely to occur than axial cracking on the inner surface around the DMW region.

Figure 20 shows the stress distribution along the DMW centerline (path B in Fig. 12). Both axial stress and circumferential stress become more compressive in the lower half thickness, which means cracks cannot grow further.

According to Fig. 2, the threshold tensile stress of alloy 182 for PWSCC initiation is about 400 MPa at 360˚C [1]. The highest tensile stress in the normal operation condition

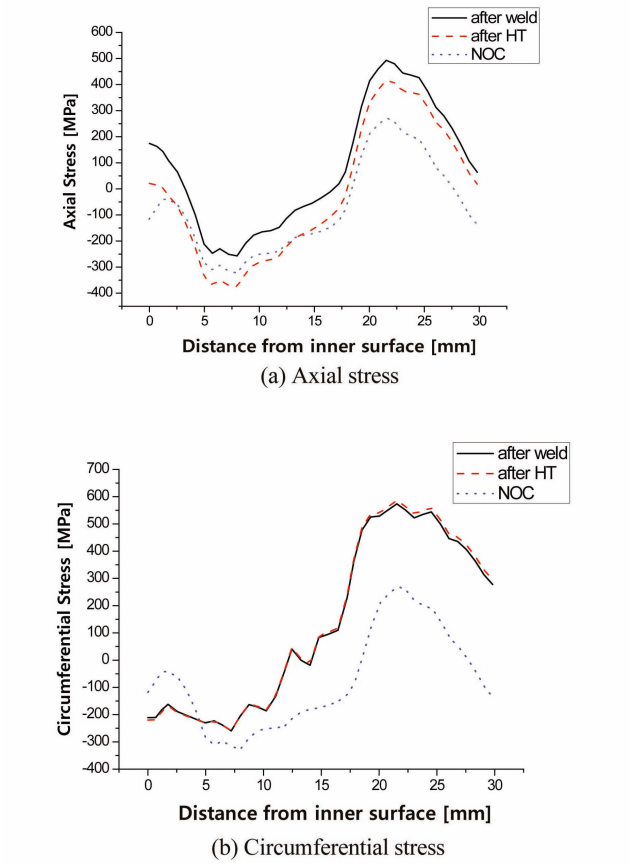

Fig. 20. Through Thickness Stress Distribution Along DMW Centerline

is about half of the threshold stress. Besides the temperature and pressure load, other piping loads exist in the plant. The piping loads should also be considered to evaluate the possibility of PWSCC initiation in the plant. The piping loads are plant specific design data and differ from plant to plant. The piping loads can be assumed to superimpose uniformly to the nozzle in the range from 35 to105 MPa [18]. If 105 MPa as piping load is assumed, the maximum axial tensile stress will be about 300 MPa.

6. CONCLUSION

The FE analysis method for weld residual stress of a nozzle was verified by comparison with mock-up measurement results. After the verification, stress conditions in the pressurizer safety nozzle in a plant were evaluated by FE analysis to evaluate PWSCC susceptibility. From the results, the fol-lowing conclusions can be made.

Large tensile residual stresses are generated by welding, especially in the axial direction in the DMW region of the pressurizer safety nozzle. Weld residual stress on the inner surface around the DMW region is alleviated by neighboring welds by more than 100 MPa. The decreasing effect from neighboring welds is more significant for axial stress than circumferential stress.

The weld residual stress changes due to constraint conditions and post- welding heat treatment to the buttering. In case When both ends were constrained (plant condition), the axial stress on the inner surface of the DMW region increased compared to the case that in which only one end is was con-strained (mock-up condition).

By hydrostatic testing, the axial stress on the inner surface of the nozzle decreased by about 100 MPa, whereas circumferential stress barely changed. The increase of temperature and pressure in-creased the circumferential stress on the inner surface of the DMW region. Axial stress was not change significantly by temperate and pressure changes.

Axial stress is more tensile than circumferential stress on the inner surface of DMW region in the pressurizer in plant operating conditions, which means circumferential cracking is more likely to occur.

According to this study, the stress value on the inner surface of the pressurizer safety nozzle un-der plant operating conditions is not high enough to initiate PWSCC. If a plant is properly welded and operated, PWSCC is not likely to occur on the surface in the pressurizer safety nozzle.

ACKNOWLEDGMENT

This work was supported by the Research Program of the Ministry of Education, Science and Technology (Mid/ Long-term Nuclear Power Research and Development Program), Republic of Korea. The title of the project was ‘Development of Analysis Technology for Crack Management of Dissimi-lar Metal Weld’ and its serial number was M207AE030001-08A0503-00110.

REFERENCES

[1] K. Ahluwalia, C. King, Review of Stress Corrosion Cracking of Alloys 182 and 82 in PWR Primary Water Service (MRP-220), October 2007

[2] D. Rudland, Y. Chen, T. Zhang, G. Wilkowski, J. Broussard and G. White, Comparison of Welding Residual Stress Solutions for Control Rod Drive Mechanism Nozzle, 2007 ASME Pressure Vessels and Piping Division Conference, July 22-26, 2007, San Antonio, TX, USA.

[3] D. Rudland, T. Zhang, G. Wilkowski, and A. Csontos, Welding Residual Stress Solutions for Dissimilar Metal Surge Line Nozzles Welds, 2008 ASME Pressure Vessels and Piping Divi-sion Conference, July 27-31, 2008, Chicago, IL, USA.

[4] T. Zhang, G. Wilkowski, D. Rudland, F. Brust, H. S. Mehta and D. V. Sommerville, Weld-Overlay Analysis – An Investigation of the Effect of Weld Sequencing, 2008 ASME Pressure Vessel and Piping Division Conference, July 27-31, 2008, Chicago, IL, USA.

[5] T. Zhang, F. Brust, G. Wilkowski, D. Rudland and A. Csontos, Welding Residual Stress and Multiple Flaw Evaluation for Reactor Pressure Vessel Head Replacement Welds with Alloy 52, 2009 ASME Pressure Vessels and Piping Division Conference, July 26-30, 2009, Prague, Czech Republic.

[6] D. Rudland, A. Csontos, F. Brust and T. Zhang, Welding Residual Stress and Flaw Evaluation for Dissimilar Metal Welds with Alloy 52 Inlays, 2009 ASME Pressure Vessels and Piping Division Conference, July 26-30, 2009, Prague, Czech Republic.
[7] Dong, P and Burst, F.W., Welding Residual Stresses and Effects on Fracture in Pressure Vessel and Piping Components : A Millenium Review and Beyond, Journal of Pressure Vessel Technology, Vol. 122 (2000), 328-338
[8] I. Sattari-Far, Y. Javadi, Influence of welding sequence on welding distortion in pipes, IJPVP 85 (2008) 265-274
[9] R.H. Leggatt, Residual stresses in welded structures, IJPVP 85 (2008) 144-151
[10] ABAQUS 6.7, Dassault Systemes Inc., 2008
[11] M. Prager, MPC Material Properties Database for ASME Division Ⅱ Rewrite, 2001-2003
[12] ASTM, Standard test method for determining residual stresses by the hole-drilling strain gage method, *ASTM E837-01, 2001*
[13] Jian Lu, Handbook of Measurement of Residual Stress, The Fairmont Press Inc. 1996
[14] K.S. Lee, T.R. Kim, J.H. Park, M.W. and Kim, S.Y. Cho, 3-D Characteristics of residual stress in the plate butt weld between SA508 and F316L SS, Journal of KSME Vol. A No.33 (2009), 401-408
[15] K.S. Lee, C.Y. Park, M.W. Kim, and J.H. Park, Distribution Characteristics of Weld Residual Stress on Butt Welded Dissimilar Metal Plate, Journal of KSME Vol. A No.34 (2010), 1317-1323
[16] Evaluation of Flaws in Austenitic Steel Piping, EPRI NP-4690-SR, July, 1986
[17] Evaluation of Flaws in Austenitic Stainless Steel Piping, Trans ASME, Journal of Pressure Vessel Technology, Vol 108, (1986) 352-366
[18] P. O'Regan, Welding Residual and Operating Stresses in PWR Alloy 82 Butt Welds (MRP-106), February, 2004